Talanta 134 (2015) 278–283

Contents lists available at ScienceDirect

Talanta

journal homepage: www.elsevier.com/locate/talanta

Laser-induced breakdown spectroscopy (LIBS) combined with hyperspectral imaging for the evaluation of printed circuit board composition

Rodrigo R.V. Carvalho, Jomarc A.O. Coelho, Jozemir M. Santos, Francisco W.B. Aquino, Renato L. Carneiro, Edenir R. Pereira-Filho *

Grupo de Análise Instrumental Aplicada (GAIA) and Grupo de Quimiometria Aplicada (GQA), Departamento de Química (DQ), Universidade Federal de São Carlos (UFSCar), PO Box 676, São Carlos, SP 13565-905, Brazil

ARTICLE INFO

Article history:
Received 21 September 2014
Received in revised form
9 November 2014
Accepted 10 November 2014
Available online 18 November 2014

Keywords:
Laser-induced breakdown spectroscopy
Waste electrical and electronic equipment
Printed circuit board
Chemometrics
Mobile phones
Scanning electron microscopy with energy-dispersive X-ray spectroscopy

ABSTRACT

In this study, laser-induced breakdown spectroscopy (LIBS) was combined with chemometric strategies (PCA, Principal Component Analysis) and scanning electron microscopy with energy-dispersive X-ray spectroscopy (SEM–EDS) to investigate the metal composition of a printed circuit board (PCB) sample from a mobile phone. Scanning electron microscopy–EDS was used for two main reasons: it was possible at the same time to visualize the sample surface, craters (made by the laser pulses) and also the chemical composition of the samples. A 30 mm × 40 mm area of the mobile phone PCB sample, which was manufactured in 2011, was investigated. In this case, a matrix with 30 rows and 40 columns (1200 points) was analyzed, and 10 pulses were performed at each point. A total of 12,000 emission spectra were recorded in the wavelength range from 186 to 1040 nm. After an initial exploratory investigation using PCA, 18 emission lines were selected (representing the elements Al, Au, Ba, Ca, Co, Cu, Fe, K, Li, Mg, Mn, Na, Ni, Sb, Si, Sn, Ti and Zn) and then normalized by the relative intensities, and a new PCA was calculated with the autoscaled data. For example, Au and Si were mainly observed in the superficial electrical contacts and in the bulk of the PCB, respectively. A second sample (a mouse PCB) was also analyzed and Pb (emission lines 357.273, 363.956, 368.346, 373.994 and 405.780 nm) was identified in the solders. In addition, this element was determined using FAAS (flame atomic absorption spectrometry) and the Pb concentration was around 25% (w/w). This study opens the possibility for improved recycling processes and the chemical investigation of solid samples measuring a few millimeters in dimension without sample preparation.

1. Introduction

Currently, the generation of waste electrical and electronic equipment (WEEE) is a major concern in EU countries and Brazil [1–3]. This type of waste is mainly composed of polymers and printed circuit boards (PCB). Printed circuit board is made of plastic material and chemical elements, mainly metals, that can be dangerous when improperly discarded. It is difficult to characterize this type of material due to its rich chemical composition, which includes a variety of elements [4]. However, the characterization of PCBs can be useful for the development of better recycling processes for the recovery of precious elements, such as Au. The size variation of PCB samples poses an additional problem; for example, mobile phones contain small PCBs, while computers contain large ones, leading to difficulty in obtaining representative samples for accurate wet sample preparation [5].

Conversely, it is also important to chemically characterize such materials in their initial life stage, specifically, when the focus of characterization is to control the quality of certain components in observation of any regulations related to public health and the environment. Taking these points into consideration, it is important to combine strategies for rapid and reliable analyses with little to no sample preparation. Laser-induced breakdown spectroscopy (LIBS) can fill this need, and when combined with chemometric strategies, this approach can solve many of the problems associated with sample characterization in this field [6–10]. Additionally, compositional mapping can be undertaken [11]. Therefore, the goal of this study is to demonstrate the use of LIBS for PCB characterization by combining hyperspectral images [12–14] and score maps obtained from principal component analysis (PCA). The use of hyperspectral images permits the simultaneous observation of the chemical distribution of multiple elements in a given sample. In a hyperspectral image [15] each pixel

* Corresponding author. Tel.: +55 16 3351 8092; fax: +55 16 3351 8350.
E-mail address: erpf@ufscar.br (E.R. Pereira-Filho).

http://dx.doi.org/10.1016/j.talanta.2014.11.019
0039-9140/

(picture element) is formed by one spectrum. In the case of LIBS each pixel has information about an emission spectrum. Energy-dispersive X-ray spectroscopy and scanning electron microscopy analyses were also performed.

2. Experimental section

2.1. Materials and equipment

In this experiment, two printed circuit boards (PCB) obtained from (1) a mobile phone manufactured in 2011 with dimensions of 30 mm × 40 mm (see details in Figs. 1 and 2) and a computer mouse with no specification (for example, year of production) were studied. There is not a particular reason to select a mobile phone manufactured in 2011, but in the authors opinion this sample is too new for a waste mobile. Both PCBs samples presented around 1–2 mm thickness and the surface was very irregular. These samples included metallic, ceramic and polymeric parts. The laser-induced breakdown spectroscopy (LIBS) system used to obtain the emission spectra was a model J200 from Applied Spectra (Freemont, USA), equipped with Axiom 2.5 software. This system is also equipped with an ablation chamber outfitted with a HEPA air cleaner, which is used to purge ablated particles, as well as an automated *XYZ* stage and a 1280 × 1024 CMOS color camera imaging system. A Nd:YAG laser (1064 nm) was used in the ablation step to deliver a maximum of 100 mJ in a single laser pulse with an 8 ns duration at a frequency of 10 Hz. The plasma light emission was guided into an optical fiber bundle coupled to a 6-channel CCD spectrometer with a spectral window ranging from 186 to 1040 nm, resulting in spectra composed of 12,288 points (variables). The Aurora software package (Applied Spectra) was employed for the identification of the emission lines. Additional conditions of operation included a gate delay of 1 μs and a gate width of 1.05 ms. To obtain semi-quantitative information from sample number 1 (the PCB from the mobile phone), a scanning electron microscope with an energy-dispersive X-ray spectroscopy unit (SEM–EDS; INSPECT F50, FEI Company, Oregon, USA) was used, and several representative parts of the sample were analyzed without any sample preparation step. In the case of sample number 2 (the PCB from the computer mouse), the solder was analyzed using flame atomic absorption spectrometry (FAAS, Thermo Scientific iCE 3000 Series AA Spectrometer, China).

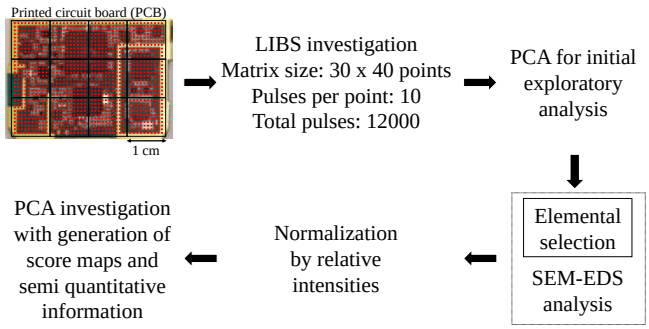

Fig. 1. Pictorial description of the data organization performed, including the following: a PCB sample, initial exploratory analysis with PCA, elemental selection and SEM–EDS analysis. The data were normalized based on the relative intensities and PCA investigation with score map generation. (For interpretation of the references to color in this figure, the reader is referred to the web version of this article.)

2.2. LIBS and SEM–EDS analyses

PCB sample number 1 was analyzed without any sample preparation, and a total of 1200 points were recorded according to the pictorial information described in Fig. 1 (see red dots). The 1200 points were organized in a matrix with 30 rows and 40

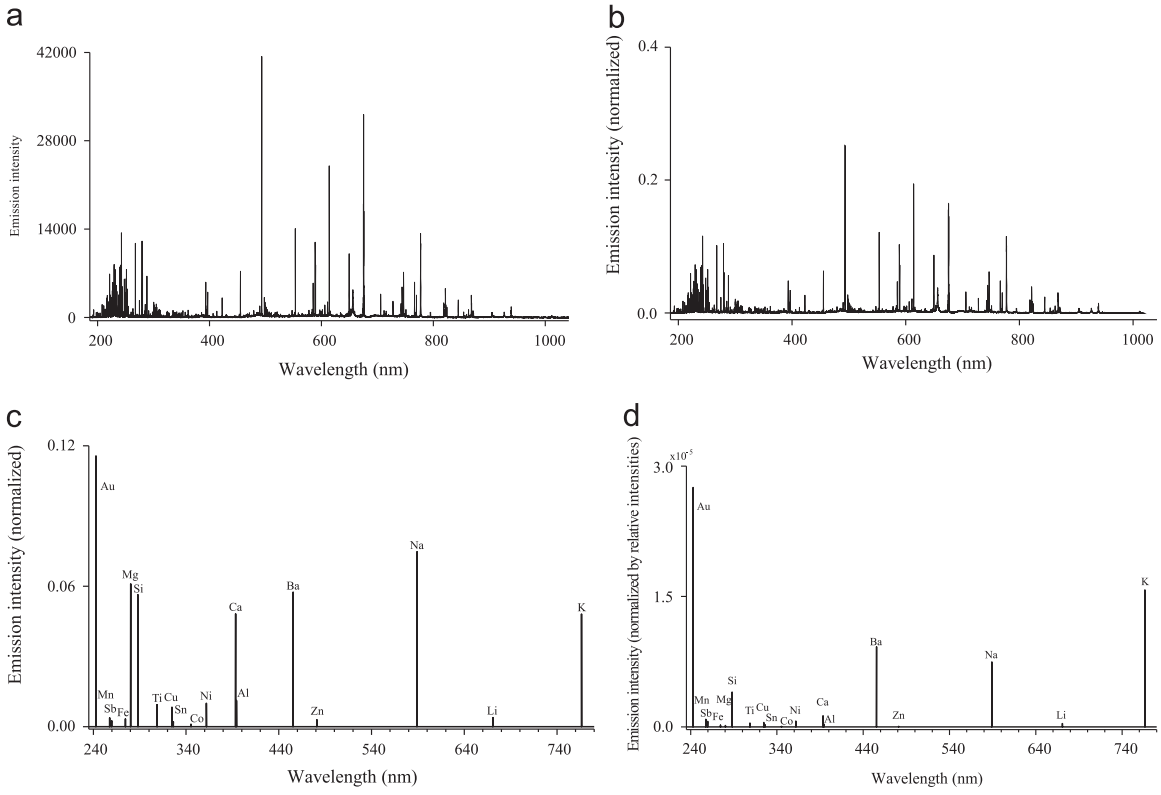

Fig. 2. The original LIBS emission spectrum (a), an emission spectrum normalized by the individual norm (b), selected emission lines (c), and the selected emission lines normalized by the relative intensities (d).

columns (30 × 40). At each point (separated by 1 mm), 10 consecutive laser pulses were performed to obtain information from both the surface and the bulk of the sample. A total of 12,000 spectra were obtained. The same sample was analyzed using SEM–EDS, and semi-quantitative information was obtained from the surface and craters formed in different representative parts of the sample (metals, ceramic and polymers). The concentrations (% w/w) of Al, Au, Ba, Ca, Co, Cu, Fe, Mg, Mn, Na, Ni, Si, Sn, Ti and Zn were recorded.

In PCB sample number 2 (from the computer mouse), a small area was analyzed, yielding a total of 75 points, which were arranged in a matrix of 5 rows and 15 columns (5 × 15). Each point was also separated by 1 mm, and a laser pulse was performed to obtain information on this solder, in particular, with regard to the presence of toxic metals, such as Pb. Additionally, for quantitative purposes, the solder was extracted, weighed and leached with a solution of aqua regia (1 ml nitric acid and 3 ml of hydrochloric acid); this combination was allowed to stand for 24 h. Finally, Pb was determined using a FAAS. The FAAS operational conditions were those recommended by the manufacturer.

2.3. Data analysis

The data set from sample number 1 was organized in a 12,000 × 12,288 matrix. Using Matlab software (version 2009a, The MathWorks, Natick, USA), the spectral information was normalized by the individual norm of each sample. The norm was calculated using

$$\text{norm} = \sqrt{\text{signal}_1^2 + \text{signal}_2^2 + \ldots + \text{signal}_n^2} \quad (1)$$

After that, each original signal was divided by its respective norm. The norm of the resulting spectra is equal to 1. Fig. 2a shows a representative spectrum in the original scale. Principal component analysis (PCA) was performed using the normalized data (Fig. 2b) to perform an initial exploratory analysis of the dataset. After this first step, 18 elements were observed in the sample. The most intense emission lines of these elements (see Fig. 2c), as identified by the PCA loadings, were recorded and divided by their respective relative intensities. This action identified the relative concentrations of the observed elements (see Fig. 2d). Table 1 shows the wavelengths and relative intensities for the 18 selected elements. Comparing Ba and Na normalized data (Fig. 2c) it is concluded, in a first glance, that the Na (0.07 normalized signal) concentration is higher than the Ba (0.06 normalized signal) concentration. On the other hand, after normalization by the relative intensity, it is observed (see Fig. 2d) that actually the Ba ($0.06/6239 = 9.6 \times 10^{-6}$) concentration is probably higher than Na ($0.07/10{,}000 = 7.0 \times 10^{-6}$). Lead was not observed in this sample. This sample probably presented an unleaded solder composed by Ag, Cu, Ni, Sn [16].

The resulting matrix (12,000 × 18) was rearranged as 10 images, each with the dimensions of 30 × 40 × 18. These 10 images were related to the order of the laser pulses, with one image obtained per pulse, from the first through the tenth pulse. This procedure was employed to evaluate the metal profile according to depth, because different numbers of layers exist in these devices. These 10 images, containing the intensities of the 18 identified elements, were autoscaled, and another PCA was performed (see details in Fig. 1). When a data is autoscaled, each signal from a single variable (x_i) is subtracted from the average ($\bar{x}$) and divided by the standard deviation (sd) that was calculated from all objects of this variable:

$$x_{auto} = \frac{x_i - \bar{x}}{\text{sd}} \quad (2)$$

The autoscaled data will have average equal to 0 and standard deviation equal to 1. In this case, the autoscaled data is shifted to the origin of the system (average = 0) and all variables have the same probability to influence the PCA analysis (standard deviation = 1).

Table 1
The selected elements and their emission lines (I: atomic and II: ionic) and relative intensities.

	Emission lines (nm)	Relative intensity
Element observed in sample 1		
Al I	394.400	33,214
Au I	242.795	4202
Ba II	455.403	6239
Ca II	393.366	37,542
Co I	345.350	13,862
Cu I	324.754	16,256
Fe II	274.648	16,103
K I	766.490	3054
Li I	670.776	10,000
Mg II	280.270	352,473
Mn II	257.610	4306
Na I	588.995	10,000
Ni I	361.939	14,900
Sb I	259.805	4002
Si I	288.157	14,058
Sn I	326.234	8374
Ti II	308.802	22,464
Zn I	481.053	37,862
Element observed in sample 2		
Pb I	357.273	16,587
Pb I	363.956	15,086
Pb I	368.346	16,954
Pb I	373.994	15,589
Pb I	405.780	25,593

We did not perform any background subtraction.

The obtained score maps and loading values were used in combination with the semi-quantitative information acquired by SEM–EDS to make assumptions about the concentrations of the elements and their positions in the sample.

In PCB sample number 2, an array (5 × 15) was obtained, and only one pulse was performed. The data were normalized by the individual norm, and the 5 most intense emission lines of Pb (see Table 1) were observed in the loading graphs; next, the graphs were compared with the images to obtain information about the presence of the same element in the solder points. The same procedure as that described previously was performed, but only 5 emission lines for Pb were used (see Table 1). This procedure was undertaken to obtain a comparison between PCB samples 1 and 2 to verify the capability of the hyperspectral imaging application to aid in the recycling process.

3. Results and discussion

3.1. Hyperspectral image interpretation

A PCA was performed for each set of 10 pulses. The score values were arranged to build score maps, which were then correlated with loading values (information regarding the analyzed elements). Fig. 3 shows the obtained results. In the initial observation, two micrographs were obtained from the metallic layer located at the superior left corner of the sample (P1, see Fig. 4). The first and second micrographs were obtained from the surface and the crater, respectively. Observing the crater, it is possible to see that after 10 laser pulses the diameter and the depth are around 100 μm (diameter) and from 10 to 20 μm (depth), respectively.

After performing a second PCA analysis with the selected and normalized emission lines, the variance was reduced.

The first principal component (PC) accounted for 19% and 16% of the original variance of the hyperspectral images of pulses 1 (Fig. 3a) and 10 (Fig. 3b), respectively.

The loading values show the information about the variables studied. In Fig. 3a, for example, Ni represent positive loading

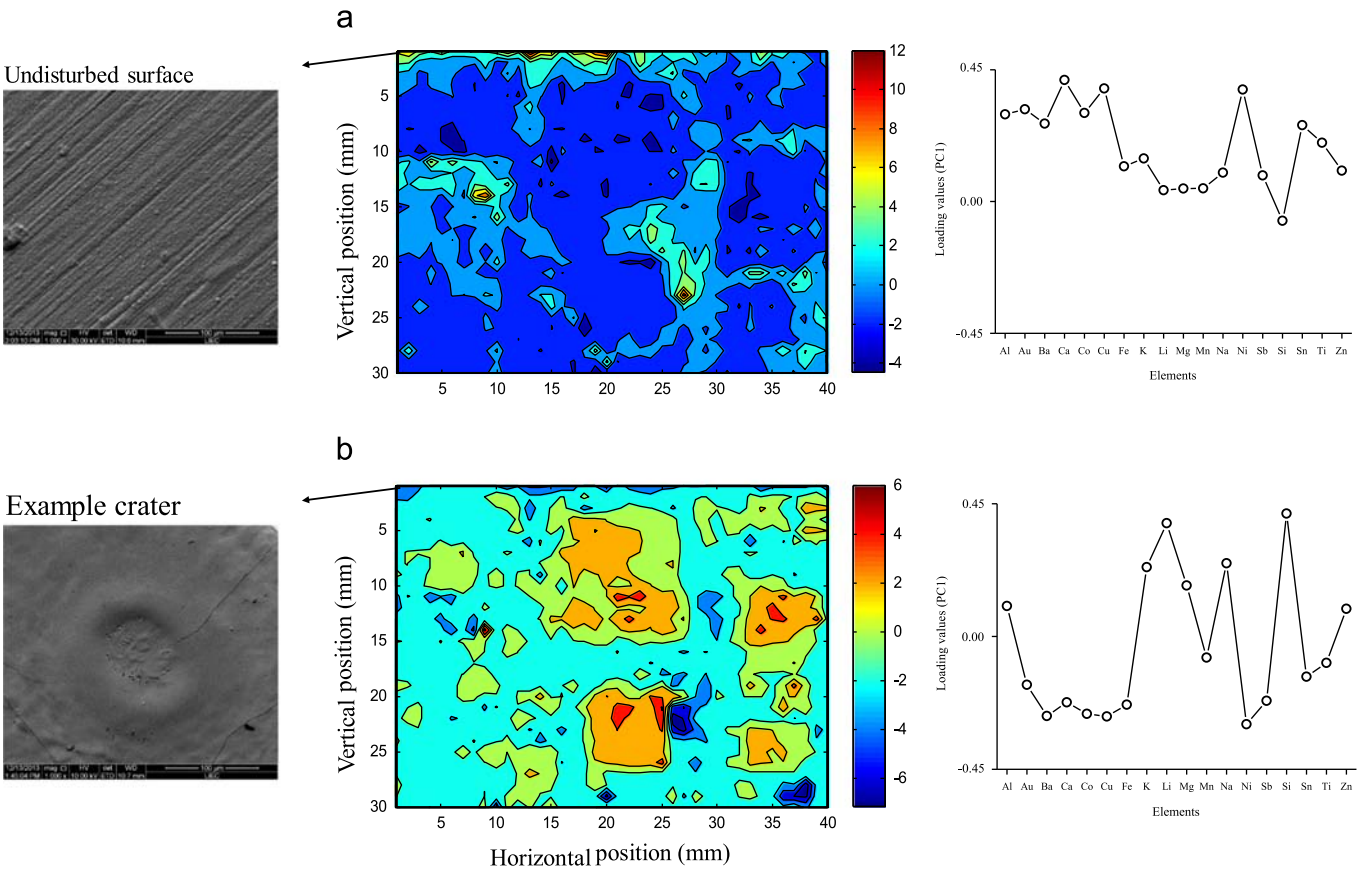

Fig. 3. Micrographs (1000 × magnification) obtained at the surface and in the crater of the sample, with score maps and loading values for pulses 1 (a) and 10 (b).

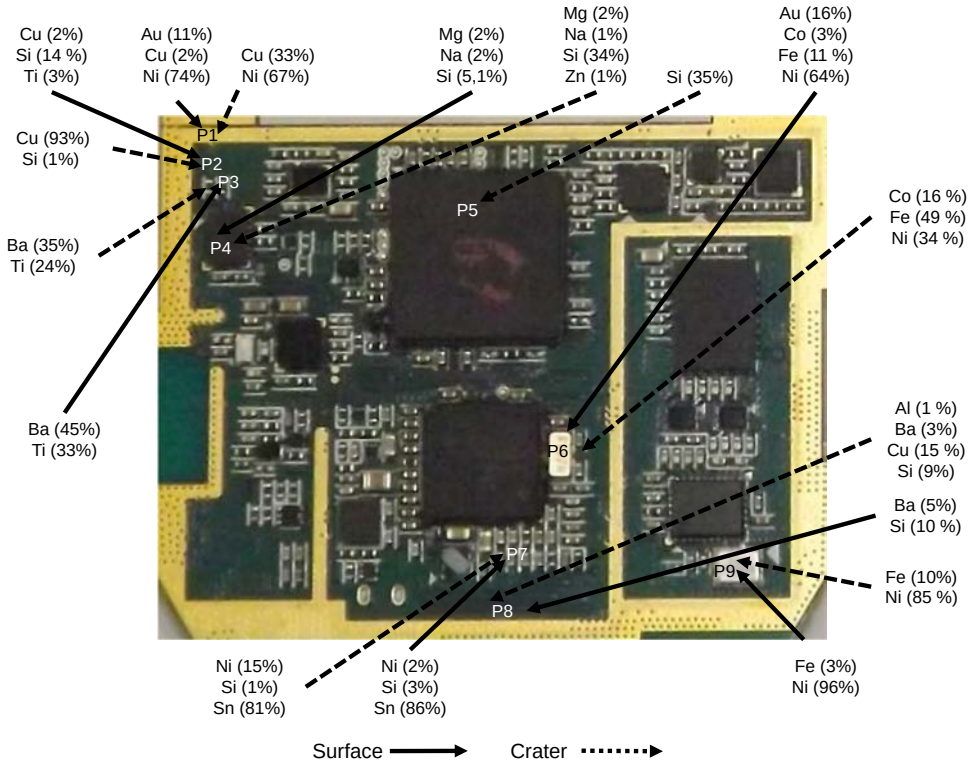

Fig. 4. Semi-quantitative information obtained using SEM–EDS for the surface (solid arrows) and crater (dotted arrows). (For interpretation of the references to color in this figure, the reader is referred to the web version of this article.)

values and this element is presented in the positive score map region (see red color). On the other hand, Si represents negative loading values and is located in the negative score map (see blue color). Another important information that needs to be mentioned is the fact that Ni and Si are inversely correlated, i.e. when the signal of Ni increases, the signal of Si decreases. In addition, the elements that represent positive loading values are positively correlated and they are presented in the same area of the sample.

In the score map for the first pulse (Fig. 3a), Si (negative loading) was the predominant constituent, as observed in the blue regions (negative scores). The other elements presented positive loading values and are related to the positive score values for the first pulse.

Fig. 4 shows selected results obtained with SEM–EDS, in which the concentrations of Au, Cu and Ni (see solid arrow) were determined to be 11%, 2% and 74% w/w, respectively, in both the upper left part of the sample (P1, see Fig. 4) and the surface. This interpretation is in accordance with the observations presented in the score map (Fig. 3a), because Au, Co, Fe and Ni represent positive loadings. Between lines 20 and 25 and columns 25 and 30 (see Fig. 3a), a region with high positive score values (a red region) can be observed. This region presents Au (16%), Co (3%), Fe (11%) and Ni (64% w/w) at the surface (P6, see Fig. 4); these results are consistent with the observations recorded in the score map for the first pulse (Fig. 3a), because Au, Co, Fe and Ni present positive loading values.

For the last pulse (pulse 10), the black polymer fraction of the sample (see Figs. 3b and 4) was observed to contain a high degree of Si (positive loading and score values). The signal inversion in some loading values did not influence the location of the analytes present in the PCB. This situation can be explained by the modification in the signs of the loadings and scores; thus, the value of the final product remains the same. This is an important consideration, because it explains how the reduction of the first set of PCA data does not lead to a loss of information regarding the metals previously detected in the same PCB portions.

In Fig. 4, the analyzed black polymer region presented a Si concentration of 35% in the crater (P5, see dotted arrow in Fig. 4). The other constituents are C and O. In Fig. 4, Au was not observed in the crater, indicating that this element is only in the surface of the sample (P1 and P6, see Fig. 4).

Other elements, such as K, Li and Sb, were also detected by LIBS, although these elements were not observed by SEM–EDS due to their low atomic numbers (K and Li) or low concentration (Sb). Lithium was mainly observed in the red regions (positive scores) of pulse 10 (see Fig. 3b). Barium, Sn and Ti were also observed at several points in the sample (P3, P7 and P8); in this case, these elements were found in the surface and in the crater.

The presence of Sb, which was readily observed in the PCB regions coated with varnish (green areas), can be explained based on its functionality: Sb increases the halogenated flame retardant action of materials. This is an interesting result following the application of this methodology, particularly in light of the difficulties in the determination of Br when using LIBS, SEM–EDS or XRF analysis. Lead was not observed.

3.2. LIBS and hyperspectral image applications

In PCBs, hyperspectral images can be used to note the location of clusters of hazardous elements. For example, in this case, Pb originating from solder is in disagreement with an ROHS directive [17,18] (see Fig. 5). In this figure, the image was obtained from a 5×15 matrix (one pulse per point separated by 1 mm) in a PCB segment from the mouse; specifically, 88% of the variance was explained by PC1. The regions with positive scores have colors that tend to be red and are assigned to the presence of Pb (see positive loadings). All Pb emission lines (see Table 1) showed positive loadings and this element is clearly related to the regions with high scores values. In the score map regions with negative scores, other elements, such as Ba, were observed. Analysis in FAAS shows a concentration of 25% (w/w) of Pb in the solder. This information is important, in light of the results from the first PCB, which indicated that the solder did not contain Pb. The recycling process entails alternative modes of segregation for the portions of materials that contain hazardous elements; for example, magnetism can be used to separate metals prior to recovery using a hydrometallurgical or pyrometallurgical process [3].

Further, the hyperspectral images obtained from electronic waste can be used in migration studies of metals and other elements from this type of residue into the environment over time, which impacts soil and groundwater. This type of approach can be performed under either real or simulated conditions, allowing for many areas affected by hazardous substances, such as Ba and Pb, to be monitored.

Many industries recover valuable metals by recycling electronics based on the formation of metallic alloys with different fractions of constituents, as previously mentioned. These alloys are resold to the producers of electronics; if certain metals are present, these low-purity alloys could result in serious industrial problems. Properties such as ductility and thermal and electrical conductivity would be affected, reducing the interest of electronic producers in these resources. LIBS and hyperspectral imaging can be applied to quality control applications when producing such alloys to evaluate the degree of purity of the metals.

4. Conclusions

This study demonstrates the application of LIBS and chemometric tools for the analysis of PCBs based on the use of PCA score maps. The positions of 18 elements were highlighted inside the sample, and the proposed method was successfully used to detect precious and toxic elements in WEEE samples, which has the potential to facilitate the efficiency of the recycling process or other sample characterization procedures.

The use of hyperspectral images can foster new routes for improved recycling processes [19], based on the combination of LIBS and chemometric techniques, which can provide the elemental distribution within a given sample. In this case, the toxic or

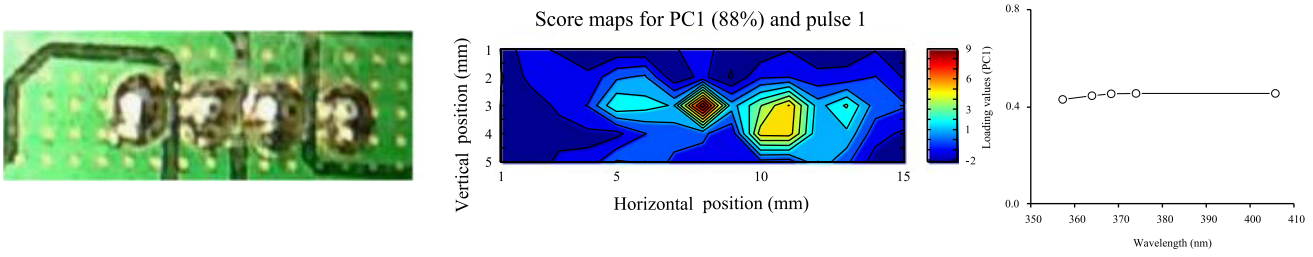

Fig. 5. Qualitative information, a score map and the loading of Pb present in the solder obtained from sample 2 (PCB from a computer mouse). (For interpretation of the references to color in this figure, the reader is referred to the web version of this article.)

precious element constituents of a sample, for example, hazardous elements such as Ba, Sb and Pb, can be segregated. Additionally, any employees who participate in the process of dismantling such materials can be better informed to use the appropriate safety devices, according to the elements detected [20]. The authors would like to stress out that the intention was to show the application of LIBS in combination with PCA (scores maps) in order to identify precious and toxic elements in PCBs. Of course 20 min (the analyses time in this case) is a long time for a single sample, but 10 pulses were performed for each point. This time interval can be reduced 10 times (2 min) if only 1 pulse is performed (information from the surface) or if several lasers are used in different directions. In addition, if a femto second laser is also used (100 Hz, for example) this time can be reduced significantly. We would like to show that the technology exists and simple mathematical (PCA) calculations can be very helpful.

Finally, no sample preparation is necessary for this technique, and the analyses were conducted directly on solid samples of small dimensions (a few centimeters).

Acknowledgments

The authors are grateful for the financial support of Conselho Nacional de Desenvolvimento Científico e Tecnológico, CNPq (Grants 304772/2012-7 and 474357/2012-0) and Grants 2012/01769-3, 2012/50827-6 and 2013/04688-7 from the São Paulo Research Foundation (FAPESP) and Thermo Scientific-Analítica for the FAAS instrument.

References

[1] O. Tsydenova, M. Bengtsson, Waste Manag. 31 (2011) 45–58.
[2] F.O. Ongondo, I.D. Williams, T.J. Cherrett, Waste Manag. 31 (2011) 714–730.
[3] L.H. Yamane, V.T. Moraes, D.C.R. Espinosa, J.A.S. Tenório, Waste Manag. 31 (2011) 2553–2558.
[4] M.A. Aguirre, M. Hidalgo, A. Canals, J.A. Nobrega, E.R. Pereira-Filho, Talanta 117 (2013) 419–424.
[5] E.M.M. Flores, J.S. Barin, J.N.G. Paniz, J.A. Medeiros, G. Knapp, Anal. Chem. 76 (2005) 3525–3529.
[6] R.E. Russo, X. Mao, J.J. Gonzalez, V. Zorba, J. Yoo, Anal. Chem. 85 (2013) 6162–6177.
[7] T. Kim, C.T. Lin, Y. Yoon, J. Phys. Chem. 102 (1998) 4284–4287.
[8] R. Noll, V. Sturm, U. Aydin, D. Eilers, C. Gehlen, M. Hohne, A. Lamott, J. Makome, J. Vrenegor, Spectrochim. Acta Part B 63 (2008) 1159–1166.
[9] R. Noll, C. Fricke-Begemann, M. Brunk, S. Connemann, C. Meinhardt, M. Scharun, V. Sturm, J. Makowe, C. Gehlen, Spectrochim. Acta Part B 93 (2014) 41–51.
[10] F.W.B. Aquino, E.R. Pereira-Filho, Analysis of the polymeric fractions of scrap from mobile phones using laser-induced breakdown spectroscopy: chemometric applications for better data interpretation, Talanta (2014), http://dx.doi.org/10.1016/j.talanta.2014.10.051 (In press).
[11] R.L. Carneiro, R.J. Poppi, Spectrochim. Acta Part A 118 (2014) 215–220.
[12] R.L. Carneiro, R.J. Poppi, J. Pharm. Biomed. Anal. 58 (2012) 42–48.
[13] R.L. Carneiro, R.J. Poppi, J. Braz. Chem. Soc. 23 (2012) 1570–1576.
[14] M. Vidal, J.M. Amigo, Chemom. Intell. Lab. Syst. 117 (2012) 138–148.
[15] P. Geladi, J. Burger, T. Lestander, Chemom. Intell. Lab. Syst. 72 (2004) 209–217.
[16] C.C. Young, J.G. Duh, S.Y. Tsai, J. Electron. Mater. 30 (2001) 1241–1248.
[17] The European Parliament and the Council of the E. Union, 37 (2003) 19–23.
[18] D. 2002/95/EC of the E.P. and of the C. on the restriction of the use of certain hazardous substances in electrical and electronic Equipment, The European Parliament and the Council of the E. Union, (2003) 24–38.
[19] H. Xia, M.C.M. Bakker, Talanta 120 (2014) 239–247.
[20] K. Hibbert, O.A. Ogunseitan, J. Hazard. Mater. 278 (2014) 1–7.